



Application of the BE subregion-by-subregion algorithm to evaluate stresses at general 3D solids and composites

F. C. de Araujo

dearaujofc@gmail.com

Universidade Federal de Ouro Preto

Campus Morro do Cruzeiro, 35400-000, Minas Gerais, Ouro Preto, Brazil

Abstract. *General solids and composites with any number of heterogeneous parts may be conveniently solved by the subregion-by-subregion (SBS) algorithm, proposed in previous works by the author. Particularly in this paper, options for calculating stresses at boundary (or interfacial) points of generic 3D solids, including composites, are incorporated into this algorithm. For that, the Hooke's law along with global-to-local axis-rotation transformations is applied. In fact, for thin-walled domains, the Hooke's law-based strategy is very relevant as nearly singular integrals are avoided. At inner points, regular boundary integration schemes are employed to evaluate stresses. Notice that the SBS-based algorithm applies to the stress analysis in any solid or composite, including the microstructural (grain-by-grain) modeling of materials. The independent assembly and algebraic manipulation of the BE matrices for the many substructures involved in the model, makes the formulation very suitable for dealing with large-order models, as typically happens in the 3D microstructural analysis of generic composites. For that, Krylov solvers are employed to construct the SBS algorithm. The performance of the technique is verified by solving complex 3D solids including representative volume elements (RVEs) of carbon-nanotube (CNT) composites with up to several tens of thousands of degrees of freedom.*

Keywords: *section properties, 3D frame element, BEM, Direct Stiffness Method*

1 INTRODUCTION

The boundary-element subregion-by-subregion (BE-SBS) technique, described in Araujo and Gray [1], and in Araujo, d’Azevedo and Gray [2], essentially consists of a robust BE-BE coupling technique based on the domain decomposition method (DDM) that allows the solution of a generic number of coupled subdomains by not explicitly assembling the subdomain submatrices into a global system of equations. To be able to do this, iterative Krylov solvers are employed, which allow the independent treatment of the many subdomains concerning the assembly of the coefficient matrices. The coupling conditions are taken into account only during the system solution.

As usually highlighted, the BEM has the advantage of requiring only the discretization of the the boundary of the domain, so that modeling solids demands much less unknowns and is by far less cumbersome than by employing domain-discretization-based methods as the FEM. In addition, in case of 3D solids consisting of many coupled parts, as for instance in composites, the BE-SBS algorithm brings about huge memory saving as the zero blocks associated with non-coupled degrees of freedom belonging to different subdomains are completely excluded. This is especially suitable for the microstructural analysis of materials, wherein grain-based models lead to huge amounts of unknowns [3]. Besides, the spontaneous way to parallelize the BE-SBS algorithm makes it a very promising tool at all for general BE-based analyses of large-order problems [4].

In this paper, a technique based on the Hooke’s law is implemented along with the BE-SBS algorithm for calculating boundary (and interfacial) stresses in 3D solids. In this technique, originally proposed in Brebbia, Telles and Wrobel [5], the boundary stresses are then evaluated by replacing the Cartesian derivatives of boundary displacement fields into stress-displacement relations. Thus, dealing with singular and quasi-singular integrals is avoided. A plate and a composite with carbon-nanotube fiber reinforcement are analyzed to verify the performance of the strategy proposed.

2 The calculation of stress

Certainly, one of the most intricate problems associated with the BEM is the efficient evaluation of singular and quasi-singular integrals. Particularly for the calculation of stresses in 3D solids, even tougher integrals have to be calculated, as the singularity order of the involved kernels is increased when compared to the one of the fundamental solution and associated derivatives. This is especially difficult for thin-walled domains as in steel structural elements wherein quasi-singular integrals take place.

To avoid then evaluating singular and quasi-singular boundary integrals involving kernels of singularity order $O(r^{-2})$ and $O(r^{-3})$, the strategy proposed in [5] is applied, which uses the Hooke’s law for the direct calculation of stresses. According to this technique, the complete stress state at solid-surface nodes referred to node-level local $\bar{x}_1, \bar{x}_2, \bar{x}_3$ Cartesian systems (see Fig. 1) is given by

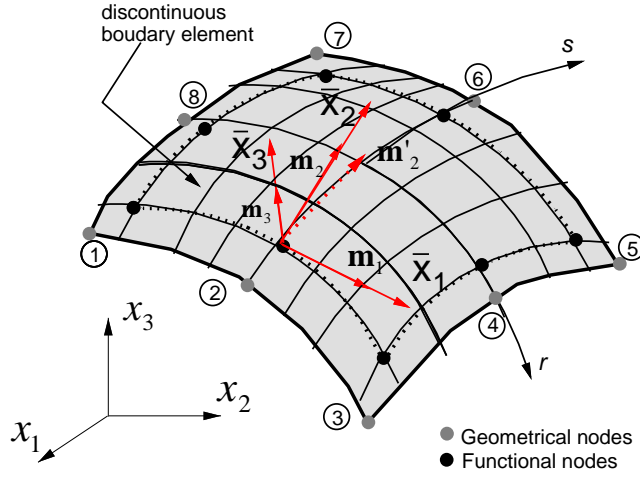


Figure 1: 3D node-level reference system

$$\left\{ \begin{array}{l} \bar{\sigma}_{11} = \left(\frac{1}{1-\nu}\right) [\nu\bar{p}_3 + 2G(\bar{\epsilon}_{11} + \nu\bar{\epsilon}_{22})] \\ \bar{\sigma}_{22} = \left(\frac{1}{1-\nu}\right) [\nu\bar{p}_3 + 2G(\bar{\epsilon}_{22} + \nu\bar{\epsilon}_{11})] \\ \bar{\sigma}_{12} = 2G\bar{\epsilon}_{12} \\ \bar{\sigma}_{13} = \bar{\sigma}_{31} = \bar{p}_1 \\ \bar{\sigma}_{23} = \bar{\sigma}_{32} = \bar{p}_2 \\ \bar{\sigma}_{33} = \bar{p}_3 \end{array} \right. , \quad (1)$$

wherein \bar{p}_1 , \bar{p}_2 , and \bar{p}_3 are the prescribed boundary tractions, ν and G are the Poisson's ratio and shear modulus respectively, and the node strains, $\bar{\epsilon}_{ij}, i, j = 1, 2$, referred to the $\bar{x}_1, \bar{x}_2, \bar{x}_3$ system, can be calculated by

$$\bar{\epsilon}_{ij} = \frac{1}{2} \left(\frac{\partial \bar{u}_i(\mathbf{x})}{\partial \bar{x}_j} + \frac{\partial \bar{u}_j(\mathbf{x})}{\partial \bar{x}_i} \right) \quad (2)$$

with Cartesian derivatives of the displacement fields given by

$$\frac{\partial \bar{u}_i(\mathbf{x})}{\partial \bar{x}_1} = \frac{\lambda_{ik}}{J(r)} \frac{\partial u_k(\mathbf{x})}{\partial r} = \frac{\lambda_{ik}}{J(r)} \left(\sum_{q=1}^{nnoel} \frac{\partial h_q(r, s)}{\partial r} u_{kq} \right) , \quad (3)$$

$$\frac{\partial \bar{u}_i(\mathbf{x})}{\partial \bar{x}_2} = \frac{1}{\bar{m}'_{22}} \left(\frac{\partial \bar{u}_i}{\partial \bar{x}'_2} - \frac{\partial \bar{u}_i}{\partial \bar{x}_1} \bar{m}'_{12} \right) , \quad (4)$$

$$\frac{\partial \bar{u}_i(\mathbf{x})}{\partial \bar{x}'_2} = \frac{\lambda_{ik}}{J(s)} \frac{\partial u_k(\mathbf{x})}{\partial s} = \frac{\lambda_{ik}}{J(s)} \left(\sum_{q=1}^{nnoel} \frac{\partial h_q(r, s)}{\partial s} u_{kq} \right) , \quad (5)$$

where $h_q(r, s)$ denotes the q -th element shape function, $J(\cdot)$ is the Jacobian associated with the Cartesian-natural coordinate transformation, $nnoel$ is the number of the nodes per element, and $\lambda_{ik} = \cos(\bar{x}_i, x_k)$. The expression 4 is needed for \bar{x}'_2 is not necessarily perpendicular to \bar{x}_1 (see

Fig. 1). The vector

$$\bar{m}'_2 = \frac{d\mathbf{l}_2}{\|d\mathbf{l}_2\|}, \quad \text{with} \quad d\mathbf{l}_2 = \frac{\partial \mathbf{x}}{\partial s}$$

is the unit tangent vector along s direction. The stress components are calculated at the geometrical contour of boundary elements, which are always continuous. In case of discontinuous elements, the displacement fields at the geometrical contour of the boundary elements are first determined via the interpolation functions for the discontinuous elements, before the stress components are calculated by the procedure above. The global stress tensor is then obtained by rotating the local stress tensor, $\bar{\sigma}$, to the global reference system via $\sigma = \mathbf{R}\bar{\sigma}\mathbf{R}^T$. Principal stresses can be eventually determined by solving the corresponding eigenvalue problem.

3 Results and discussion

To verify the strategy proposed, a 3D analysis of a plate under bending and of a carbon-nanotube (CNT) reinforced composite is carried out by means of the BE-SBS-based code, and stresses are measured at boundary (or interfacial) nodes. To compare the results, the problems are also analyzed by using the ANSYS 13 software.

3.1 Thick plate under bending

A square plate with side length $l = 3m$ and thickness $t = 10cm$, clamped at all sides and along a strip on its inferior surface (see Fig. 2(a)) is solved for a distributed load of $q = 10 kN/m^2$. Stresses are measured at boundary nodes along lines on the top and bottom surfaces of the plate (superior and inferior lines respectively). For that, the BE-SBS model shown in Fig. 2(b), with 4,614 degrees of freedom is considered. The corresponding ANSYS model contains 20,175 degrees of freedom.

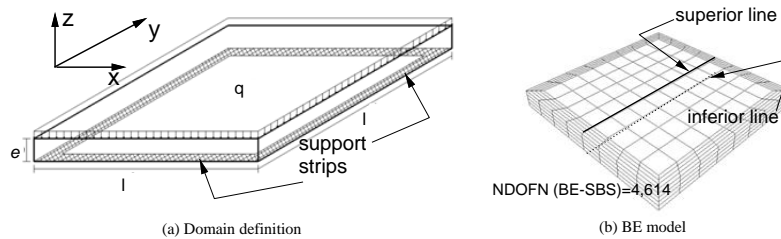


Figure 2: 3D square thick plate

Results for the σ_{xx} component on boundary nodes located at the superior and inferior lines of the plate surface, calculated using the BE-SBS-based code and the ANSYS software, are given in Table 1 and Fig. 3(a) for the superior line, and in Fig. 3(b) for the inferior line. With the exception of special points around the support strips, an excellent agreement between the calculations employing the BE-SBS and the ANSYS software is verified. In fact, in those points around the support strips (at the bottom plate surface), σ_{xx} is expected to be singular, and the BEM is able to reconstitute this behavior.

Table 1: σ_{xx} (kN/m^2) along the superior and inferior lines

x coordinate (m)	superior line		inferior line	
	BE-SBS	ANSYS 13	BE-SBS	ANSYS 13
0.100	31.67	31.97	-9.48	-73.37
0.150	66.00	58.58	-67.67	-23.71
0.200	94.65	73.37	-482.70	-151.18
0.525	-34.60	-86.28	-26.04	-22.53
0.850	-108.21	-102.61	59.19	55.69
1.175	-146.07	-142.41	102.67	98.83
1.500	-155.81	-153.01	115.75	111.38
1.825	-146.07	-142.41	103.72	98.83
2.150	-110.87	-102.61	62.12	55.69
2.475	-34.60	-86.28	-26.05	-22.53
2.800	108.56	73.37	-482.70	-151.18
2.850	67.19	58.58	-67.67	-23.71
2.900	34.72	31.97	-9.48	-73.37

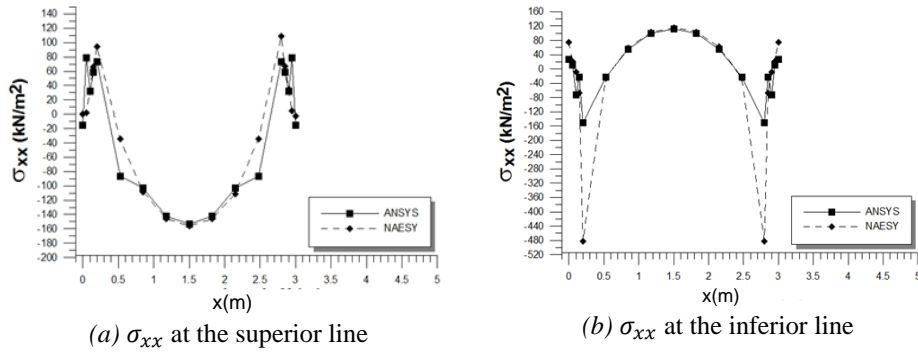


Figure 3: Normal stress σ_{xx} at plate-surface points

3.2 CNT representative volume element (RVE)

In this problem, stresses are measured in representative volume elements (RVEs) of polymeric composites reinforced with short carbon-nanotube (CNT). In this problem, the RVEs shown in Fig. 4(a) and (b), with one and 4 unit cells respectively, are considered. The dimensions of each unit cell are $l_1 = 100 \text{ nm}$ (length), $l_2 = l_3 = 20 \text{ nm}$ (side lengths of the cross-section), and the short CNT (inside the polymeric matrix) is 50 nm long (including the hemispherical caps), and the radii of its cylindrical part and hemispherical caps are $r_0 = 5.0 \text{ nm}$ and $r_i = 4.6 \text{ nm}$, characterizing a thin shell. The material properties are $E_{CNT} = 1,000 \text{ nN/mm}^2$, $\nu_{CNT} = 0.3$ (for the CNT) and $E_m = 100 \text{ nN/mm}^2$, $\nu_m = 0.3$ (for the polymeric material), and the loading state is defined by an axial unit displacement (see Chen and Liu [6], and Araujo, d’Azevedo and Gray [4]). The comparison of the stress values with those presented in [6] (calculated by employing 3D FE models) are good, although in that paper no numerical values for stress components are given, and the comparison was done only qualitatively by observing the color graphs. However to show the correctness of the results, numerical values of the effective elasticity modulus and Poisson’s ratio for CNT-based RVE are compared with those furnished in [6] and show in in Table 2 attesting excellent agreement.

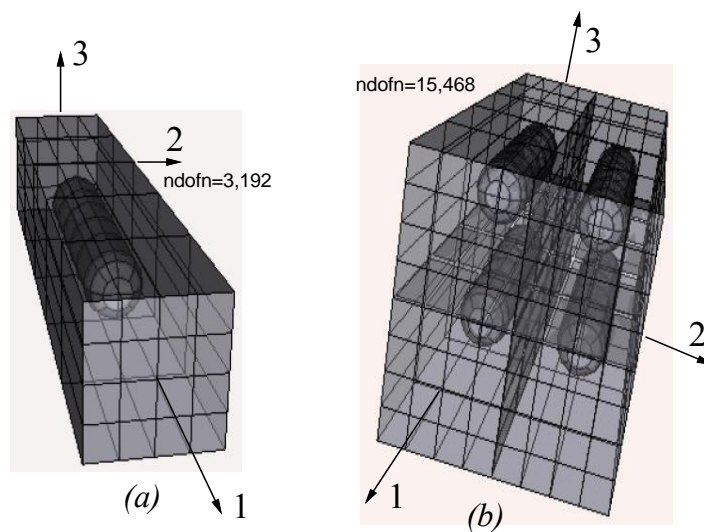


Figure 4: BE models for the CNT-reinforced composites

Table 2: Material constants for the short-CNT-based RVEs

model	E_1/E_m	$E_2/E_m = E_3/E_m$	ν_{12}, ν_{13}	ν_{23}
1×1	1.0378	0.9366	0.2963	0.3207
2×2	1.0379	0.9379	0.2976	0.3217
Chen & Liu (3D FE)	1.0391	0.9342	0.3009	0.3217

4 Conclusions

The results obtained with the present strategy show good efficiency for evaluating boundary (or interfacial) stresses in 3D solids. By employing this technique, the evaluation of integrals of O^{-2} and O^{-3} singular kernels are avoided, what is very suitable for thin-walled solid parts. In fact, the implementation of that strategy in the frame of the BE-SBS code, allowed the analysis of the complex 3D short-CNT-based RVEs in Fig. 4. On the other hand, by comparing the FE model in [6] (just for one single cell) with those in Fig. 4, we see that the BE models are by far less cumbersome than those employed by Chen and Liu [6].

Ackowlegments

This research has been sponsored by the Brazilian Research Council (CNPq), the Coordination for Improvement of Higher-Education Personnel (CAPES), and the Universidade Federal de Ouro Preto (UFOP).

Bibliography

- [1] F. C. Araujo, L. J. Gray. (2008). *Evaluation of effective material parameters of CNTreinforced composites via 3D BEM*. CMES, v 24, p. 103-121.
- [2] F.C. Araujo, E.F. dAzevedo, L.J. Gray (2011). *Constructing efficient substructure-based preconditioners for BEM systems of equations*. Eng. Anal. Boundary Elements, 35, 517526.
- [3] I. Benedetti, M.H. Aliabadi. (2013). *Three-dimensional grain boundary formulation for microstructural modelling of polycrystalline materials*. Computational Materials Science, 67, 249-260.
- [4] F.C. Araujo, E.F. dAzevedo, L.J. Gray (2010). *Boundary-element parallel-computing algorithm for the microstructural analysis of general composites*. Computers & Structures, 88, 773-784.
- [5] C. A. Brebbia, J. C. F. Telles, L.C. Wrobel (1984). *Boundary element techniques: theory and applications in engineering*. Springer-Verlag, Berlin.
- [6] X.L. Chen, Y.J. Liu. (2004). *Square representative volume elements for evaluating the effective material properties of carbon nanotube-based composites*. Comput. Mat. Sci.,29, 111.